DeepGraphMol, a multi-objective, computational strategy for generating molecules with desirable properties: a graph convolution and reinforcement learning approach

[1,2]Yash Khemchandani, [3]Stephen O'Hagan, [1]Soumitra Samanta, [1]Neil Swainston, [1]Timothy J. Roberts, [4]Danushka Bollegala & [1,5,*]Douglas B. Kell

[1]Department of Biochemistry and Systems Biology, Institute of Systems, Molecular and Integrative Biology, University of Liverpool, Crown St, Liverpool L69 7ZB, UK.

[2]Indian Institute of Technology Bombay, Powai, Mumbai 400 076, Maharashtra, India

[3]Dept of Chemistry, Manchester Institute of Biotechnology, The University of Manchester, 131 Princess St, Manchester M1 7DN, UK.

[4]Dept of Computer Science, University of Liverpool, Ashton Building, Ashton Street, Liverpool, L69 3BX, UK.

[5]The Novo Nordisk Foundation Center for Biosustainability, Technical University of Denmark, Kemitorvet 200, 2800 Kgs Lyngby, Denmark.

***Correspondence:** Douglas B. Kell, dbk@liv.ac.uk http://dbkgroup.org/ @dbkell

Keywords: Cheminformatics – deep learning – generative methods – QSAR – reinforcement learning

DeepGraphMol, a multi-objective, computational strategy for generating molecules with desirable properties: a graph convolution and reinforcement learning approach . 1

Abstract 2

1 Introduction 3

2. Methods 4

2.1 Molecular Property Prediction 5

2.1.1 Feature Extraction 5

2.1.2 Regression 6

2.2 Reinforcement Learning for Molecular Generation 7

2.2.1 Molecular Representation 7

2.2.2 Reinforcement Learning setup 7

2.2.3 Graph Convolutional Policy Network 8

2.2.4 Policy Gradient Training 10

3. System evaluation 11

3.1 Property Prediction 11

3.1.1 Hyperparameter Optimization 12

3.1.2 Implementation details 13

3.3 Multi-Objective Molecular Generation 18

Conclusions 20

Acknowledgments 20

References 20

Abstract

We address the problem of generating novel molecules with desired interaction properties as a multi-objective optimization problem. Interaction binding models are learned from binding data using graph convolution networks (GCNs). Since the experimentally obtained property scores are recognised as having potentially gross errors, we adopted a robust loss for the model. Combinations of these terms, including drug likeness and synthetic accessibility, are then optimized using reinforcement learning based on a graph convolution policy approach. Some of the molecules generated, while legitimate chemically, can have excellent drug-likeness scores but appear unusual. We provide an example based on the binding potency of small molecules to dopamine transporters. We extend our method successfully to use a multi-objective reward function, in this case for generating novel molecules that bind with dopamine transporters but not with those for norepinephrine. Our method should be generally applicable to the generation *in silico* of molecules with desirable properties.

1 Introduction

The *in silico* (and experimental) generation of molecules or materials with desirable properties is an area of immense current interest (e.g. [1-28]). However, difficulties in producing novel molecules by current generative methods arise because of the discrete nature of chemical space, as well as the large number of molecules [29]. For example, the number of drug-like molecules has been estimated to be between 10^{23} and 10^{60} [30-34]. Moreover, a slight change in molecular structure can lead to a drastic change in a molecular property such as binding potency (so-called activity cliffs [35-37]).

Earlier approaches to understanding the relationship between molecular structure and properties used methods such as random forests [38, 39], shallow neural networks [40, 41], Support Vector Machines [42], and Genetic Programming [43]. However, with the recent developments in Deep Learning [44, 45], deep neural networks have come to the fore for property prediction tasks [3, 46-48]. Notably, Coley *et al*. [49]] used Graph convolutional networks effectively as a feature encoder for input to the neural network.

In the past few years, there have been many approaches to applying Deep Learning for molecule generation. Most papers use the Simplified Molecular-Input Line-Entry System (SMILES) strings as inputs [50], and many use a Variational AutoEncoder architecture (e.g. [3, 17, 51]), with Bayesian Optimization in the latent space to generate novel molecules. However, the use of a sequence-based representational model has a specific difficulty, as any method using them has to learn the inherent rules, in this case of SMILES strings. More recent approaches, such as Grammar Variational AutoEncoders [52, 53] have been developed in attempts to overcome this problem but still the molecules generated are not always valid. Some other approaches try to use Reinforcement Learning for generating optimized molecule [54]. However, they too make use of SMILES strings which as indicated poses a significant problem. In particular, the SMILES grammar is entirely context-sensitive: the addition of an extra atom or bracket can change the structure of the encoded molecule dramatically, and not just 'locally' [55].

Earlier approaches have tended to choose a specific encoding for the molecules to be used as an input to the model, such as one hot encoding [56, 57], Extended Connectivity Fingerprints [58, 59] and SMILES strings directly. We note that these encodings do not necessarily capture the features that need to be obtained for prediction of a specific property (and all encodings extract quite different and orthogonal features [60]).

In contrast, the most recent state-of-the-art methods, including hypergraph grammars [61], Junction Tree Variational Auto Encoders [62] and Graph Convolutional Policy Networks [34], use a graphical representation of molecules rather than SMILES strings and have achieved 100% validity in molecular generation. Graph-based methods can be seen as a more natural representation of molecules as substructures map directly to subgraphs, but subsequences are usually meaningless. However, these have only been used to compare the models on deterministic properties such as the Quantitative Estimate of Drug-likeness (QED) [63], logP, etc. that can be calculated directly from molecular structures (e.g. Using RDKit, http://www.rdkit.org/). For many other applications, molecules having a higher score for a specific *measured* property are more useful. We here try to tackle this problem.

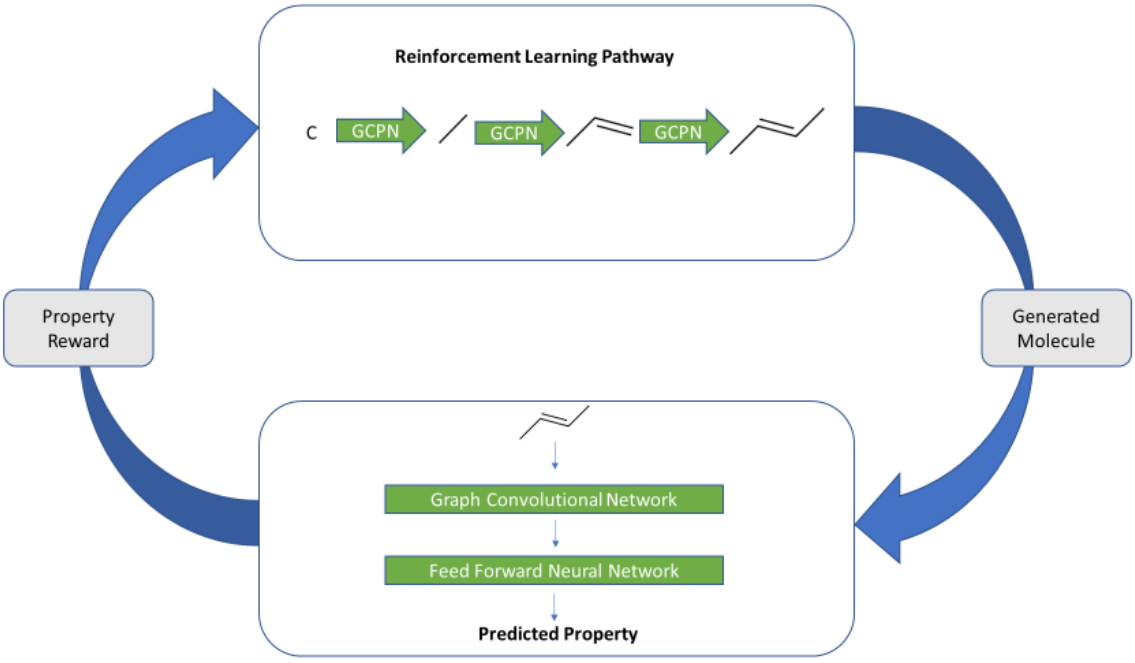

Figure 1. Block diagram of our basic system. A molecule is generated by the Reinforcement Learning (RL) pathway using a Graph Convolutional Policy Networks. This molecule is then used as an input for the property prediction module which outputs the property score as predicted by the module. This score is then used as the reward feedback for the RL pathway and the cycle restarts

2. Methods

Our system consists of two parts: Property Prediction and Molecular Generation. For both the parts, we represent the molecules as graphs [64] since they are a more natural representation than are SMILES strings, and substructures are simply subgraphs. We train a model to predict the property scores of the molecules, specifically the binding constant of various molecules at the dopamine and norepinephrine transporters (using a dataset from BindingDB). The first part, used for (training) the property prediction part, is a Graph Convolutional Network as a feature encoder together with a Feed Forward Network. We also use an Adaptive Robust Loss Function (as suggested by [65]) since the experimental data are bound to be error prone. For the Molecular Generation task, we use the method proposed by You and colleagues [34]. In particular, we (and they) use Reinforcement Learning for this task since it allows us to incorporate both the molecular constraints and the desired properties using reward functions. This part uses graph convolution policy networks (GCPNs), a model consisting of a GCN that predicts the next action (policy) given the molecule state. It is further guided by expert pretraining and adversarial loss for generating valid molecules. Our code (https://github.com/dbkgroup/prop_gen) is essentially an integration of the property prediction code of Yang and colleagues [66, 67] (https://github.com/swansonk14/chemprop) and the reinforcement learning code provided by You and colleagues [34].

2.1 Molecular Property Prediction

As noted, the supervised property prediction model consists of a graph-convolution network for feature extraction followed by a fully interconnected feedforward network for property prediction.

2.1.1 Feature Extraction

We represent the molecules as directed graphs, with each atom (i) having a feature vector F_i ($\mathbb{R}^{133}$) and each bond (between atom i & j) having feature vector F_{ij} ($\mathbb{R}^{14}$). For each incoming bond a feature vector is obtained by concatenating the feature vector of the atom to which the bond is incoming and the feature vector of the bond. Thus the input tensor is of the size N_{bonds} x $\mathbb{R}^{147}$. The Graph Convolution approach allows the message (feature vector) for a bond to be passed around the entire graph using the approach described below.

The initial atom-bond feature vector that we use incorporates important molecular information that the GCN encoder can then incorporate in later layers. The initial representations for the atom and bond features are taken from https://github.com/swansonk14/chemprop and summarized in Table 1, below. Each descriptor is a one-hot vector covering the index-range represented by it (except the Atomic Mass). For Atomic Number, Degree, Formal Charge, Chiral Tag, Number of Hydrogens and Hybridization, the feature vector contains one additional dimension to allow uncommon values (values not in the specified range).

INDICES	**ATOM DESCRIPTION**
0 – 100	Atomic Number (1 to 100)
101-107	Degree (1 to 5)
108-113	Formal Charge (-2 to + 2)
114-118	Chiral Tag (0 to 4)
119-124	Number of Hydrogens (0 to 4)
125-130	Hybridization (SP, SP2, SP3, SP3D, SP3D2)
131	Aromatic Atom
132	Atomic Mass * 0.01
INDICES	**BOND DESCRIPTION**
133	Bond Present
134-136	Bond Type (Single, Double, Triple)
137	Aromatic Bond
138	Conjugated Bond
139	Bond present in Ring
140-146	Bond Stereo Code (RdKit)

Table 1. Atom and bond features used in the present work

The initial atom-bond feature vector is then passed through a linear layer followed by ReLU Activation [68, 69] to get the Depth-0 message vector for each bond. For each bond, the message vectors for the neighbouring bonds are summed up (Convolution step) and passed through a linear layer followed by ReLU and a Dropout layer to get the Depth-1 message vectors. This process is continued up to a specified Depth-(N-1) message vectors. To get the Depth-N message vectors, the Depth-(N-1) vectors of all the incoming bonds for an atom are summed and then passed through a dense layer followed by ReLU and Dropout. The final graph embedding for the molecule is obtained by averaging the depth-N message vectors over all the atoms. The exact details for this model can be found in section 3.1.1.

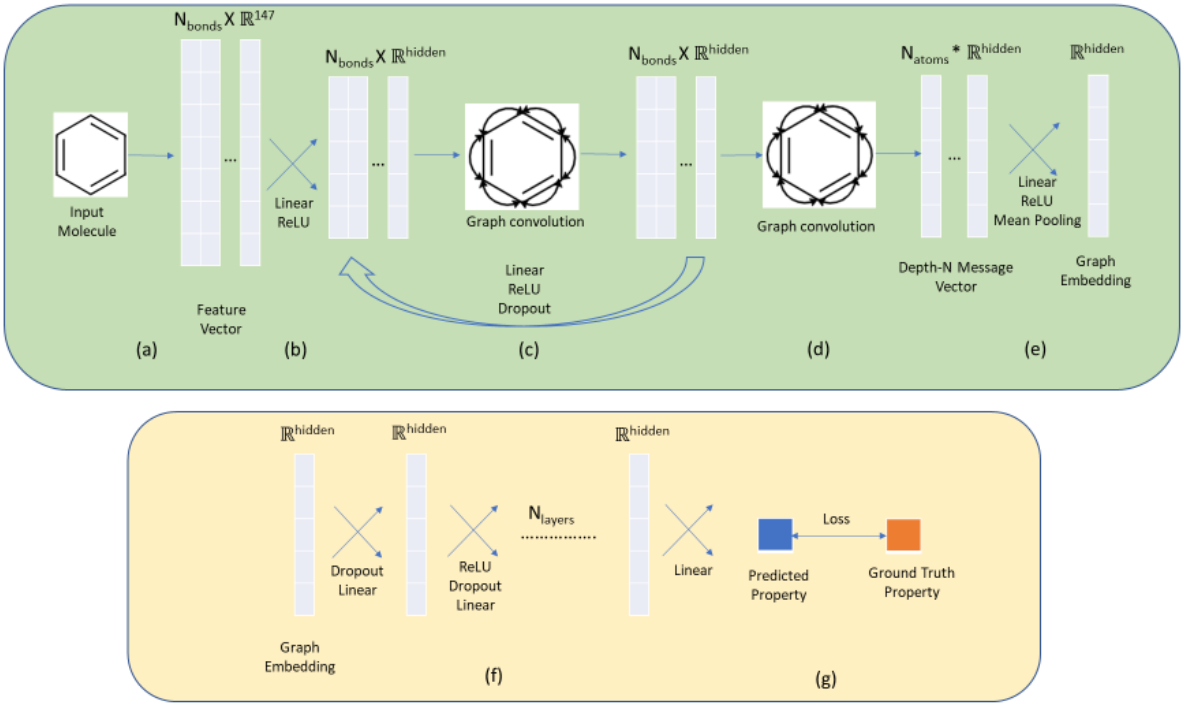

Figure 2. The property prediction pipeline for our method. The steps in green represent the feature extraction using Graph Convolution and the steps in orange represent regression of property scores. (a) The molecule is represented is a feature vector with features described as in section 2.1. (b) The feature vector is passed through a linear layer to get Depth-0 message. (c) Through repeated graph convolution (message passing) followed by Linear Layer, we get Depth N-1 message. (d) Each atom's final message is calculated by summing up the messages (also Graph Convolution) of the neighbouring atoms. (e) The resultant message is passed through a Linear Layer and the mean of all the atoms is taken to get the final embedding. (f) The property score is regressed from the graph embedding by a Feed Forward Neural Network. (g) The loss between predicted property and ground truth property is then backpropagated to change the weights.

2.1.2 Regression

To perform property prediction the embedding extracted by the GCN is fed into a fully connected network. Each intermediate layer consists of a Linear Layer followed by ReLU activation and Dropout that map the hidden vector to another vector of the same size. Finally the penultimate nodes are passed through a Linear Layer to output the predicted property score. The K_i values present in the dataset were obtained experimentally so might contain experimental errors. If we were to train our model with a simple loss function such as root mean square (RMS) error loss, it would not be able to generalize well because of the presence of outliers in the training set. Overcoming this problem requires training the data with the help of a robust loss function that takes care of the outliers present in the training data. There are several types of robust loss functions such as Pseudo-Huber loss [70], Cauchy loss, etc., but each of them has an additional hyperparameter value (for example δ in Huber Loss) which is treated as a constant while training. This means that we have to manually tune the hyperparameter each time we train to get the optimum value which may result in extensive training time. To overcome this problem , as proposed by [65], we have used a general robust loss function

that has the hyperparameters as shape parameter (α) which controls the robustness of the loss, and the scale parameter (c) which controls the size of the loss's quadratic bowl near x=0. This loss is dubbed as a "general" loss since it takes the form of other loss functions for particular values of α. (e.g L2 loss for α=2, Charbonnier loss for α=1, Cauchy loss for α=0). The authors also propose that "by viewing the loss function as the negative log likelihood of a probability distribution, and by treating robustness of the distribution as a latent variable" we can use gradient-based methods to maximize the likelihood without manual parameter tuning. In other words, we can now train the hyperparameters α and c rather which overcomes the earlier problem of manually tuning the hyperparameters. The loss function and the corresponding probability distribution are described in Eq. 1 and Eq. 2 respectively.

$$f(x,\alpha,c) = \frac{|\alpha-2|}{\alpha}\left(\left(\frac{(x/c)^2}{|\alpha-2|}+1\right)^{\alpha/2}-1\right) \qquad \text{Eq. 1}$$

$$p(x|\alpha,c) = \frac{1}{cZ(\alpha)}\exp\big(-f(x,\alpha,c)\big)$$
$$Z(\alpha) = \int_{-\infty}^{\infty}\exp\left(-f(x,\alpha,1)\right) \qquad \text{Eq. 2}$$

2.2 Reinforcement Learning for Molecular Generation

2.2.1 Molecular Representation

We follow the method described by the GCPN paper [34] for the molecular generation task, with the difference being that the final property reward is the value calculated by the previously trained model for the newly generated molecules. As in the previous part, we represent the molecules as graphs, more specifically as (A, E, F) where $A \in \{0,1\}^{n\times n}$ is the adjacency matrix, $F \in \mathbb{R}^{n\times d}$ is the node (atom) feature matrix and $E \in \{0,1\}^{3\times n\times n}$ is the edge-conditioned adjacency tensor (since the number of bond-types is 3, namely single, double and triple bond), with n being the number of atoms and d being the length of feature vector for each atom. More specifically, $E_{i,j,k} = 1$ if there exists a bond of type i between atoms j and k , and $A_{j,k} = 1$ if there exists any bond between atoms j and k.

2.2.2 Reinforcement Learning setup

Our model environment builds a molecule step by step with the addition of a new bond in each step. We treat graph generation as a Markov Decision Process such that the next action is predicted based only on the current state of the molecule, not on the path that the generative process has taken. This reduces the need for sequential models such as RNNs and the disadvantages of vanishing gradients associated with them, as well as reducing the memory load on the model. More specifically, the decision process follows the equation: $p\,(s_{t+1}\,|s_t,\ldots s_0\,) = p(s_{t+1}|s_t\,)$, where p is the probability of the next state (s_{t+1}) given the previous state (s_t).

We can initialize the generative process with either a single C atom (as in Experiments 1 and 2) or with another molecule (as in Experiments 3, 4 and 5). At any point in the generation process, the state of the environment is the graph of the current molecule that has been built up so far. The action space is a vector of length 4 which contains the information – First Atom, Second Atom, Bond type and Stop. The stop signal is either 0 or 1 indicating whether the generation is complete, based on valence rules. If the action defies the rules of chemistry in the resultant molecule, the action is not considered and the state remains as it is.

We make use of both intermediate and final rewards to guide the decision-making process. The intermediate rewards include stepwise validity checks such that a small constant value is added to the reward if the molecule passes the valency checks. The final reward includes the pK_i value of the final molecule as predicted by the trained model and the validity rewards (+1 for not having any steric strain and +1 for absence of functional groups that violate ZINC functional group filters). Two other metrics are the quantitative estimation of drug-likeness (QED) [63] and the synthetic accessibility (SA) [71] score. Since our final goal is to generate drug-like molecules that can be synthetically generated, we also add the QED and 2*SA score of the final molecule to the reward.

Apart from this, we also use adversarial rewards so that the generated molecules resemble (prediction) the given set of molecules (real). We define the adversarial rewards $V(\pi_\theta, D_\Phi)$ in Eq 3.

$$\min_{\theta} \max_{\phi} V(\pi_\theta, D_\phi) = E_{x\sim p_{\text{data}}}[\log D_\phi(x)] + E_{x\sim \pi_\theta}[\log D_\phi(1-x)] \qquad \text{Eq. 3}$$

where π_θ is the policy network, D_φ is the discriminator network, x represents the input graph and p_{data} is the underlying data distribution which is defined either over final graphs (for final rewards) or intermediate graphs (for intermediate rewards) (just as proposed by You and colleagues [34]). Alternate training of generator (policy network) and discriminator by gradient descent methods will not work in our case since x is a non-differentiable graph object. Therefore we add $-V(\pi_\theta, D_\Phi)$ to our rewards and use policy gradient methods [72] to optimize the total rewards. The discriminator network comprises a Graph Convolutional Network for generating the node embedding and a Feed Forward Network to output whether the molecule is real or fake. The GCN mechanism is same as that of the policy network which is described in the next section.

2.2.3 Graph Convolutional Policy Network

We use Graph Convolutional Networks (GCNs) as the policy function for the bond prediction task. This variant of graph convolution performs message passing over each edge type for a fixed depth L. "The node embedding for the next depth ($l + 1$) is calculated as described in Eq. 4

$$H^{(l+1)} = \text{AGG}\left(\text{ReLU}\left(\{\tilde{D}_i^{\frac{-1}{2}} \tilde{E}_i \tilde{D}_i^{\frac{-1}{2}} H^{(l)} W_i^{(l)}\}, \forall i \in (1, \dots, b)\right)\right) \qquad \text{Eq. 4}$$

where E_i is the ith slice of the tensor E , $\tilde{E}_i = E_i + I$, $\widetilde{D}_i = \sum_k \tilde{E}_{ijk}$, $W_i^{(l)}$ is a trainable weight matrix for the ith edge type, and $H^{(l)}$ is the node embedding learned in the lth layer with $H^{(l)} \in \mathbb{R}^{(n+c)\times d}$ [34]. n is the number of atoms in the current molecule and c is the number of possible atom types (C,N,O etc.) that can be added to the molecule (one atom is added in each step) with d representing the dimension of the embedding. We use mean over the edge features as the Aggregate (AGG) function to obtain the node embedding for a layer. This process is repeated L times until we get the final node embedding.

This node embedding X is then used as the input to four Multilayer Perceptrons (MLP, denoted by m), that map a matrix $Z \in \mathbb{R}^{p\times d}$ to $\mathbb{R}^p$ representing the probability of selecting a particular entity from the given p entities. The specific entity is then sampled from the probability distribution thus obtained. Note that since the action space is a vector of length 4, we use 4 perceptrons to sample each component of the vector. The first atom has to be from the current molecule state while the second atom can be from the current molecule (forming a cycle) or a new atom outside the molecule (adding a new atom). For selecting the first atom, the original embedding X is passed to the MLP m_f and outputs a vector of length equal to n. While selecting the second atom, the embedding of the first atom $X_{a_{\text{first}}}$ is concatenated to the original embedding X and passed to the MLP m_s giving a vector of length equal to $n + c$. While selecting the edge type, the concatenated embedding of the first ($X_{a_{\text{first}}}$) and second ($X_{a_{\text{second}}}$) atom is used as an input to MLP m_e and outputs a vector of length equal to 3 (number of bond types). Finally, the mean embedding of the atoms is passed to MLP m_t to output a vector of length 2 indicating whether to stop the generation. This process is described in equations 5-9.

$$a_t = \text{CONCAT}\left(a_{\text{first}}, a_{\text{second}}, a_{\text{edge}}, a_{\text{step}}\right) \qquad \text{Eq. 5}$$

$$f_{\text{first}}(s_t) = \text{SOFTMAX}\left(m_f(X)\right) \qquad a_{\text{first}} \sim f_{\text{first}}(s_t) \in \backslash\{0,1\backslash\}^n \qquad \text{Eq. 6}$$

$$f_{\text{second}}(s_t) = \text{SOFTMAX}\left(m_s\left(X_{a_{first}}, X\right)\right) \qquad a_{\text{second}} \sim f_{\text{second}}(s_t) \in \backslash\{0,1\backslash\}^{n+c} \qquad \text{Eq. 7}$$

$$f_{\text{edge}}(s_t) = \text{SOFTMAX}\left(m_e\left(X_{a_{\text{first}}}, X_{a_{\text{second}}}\right)\right) \qquad a_{\text{edge}} \sim f_{\text{edge}}(s_t) \in \backslash\{0,1\backslash\}^b \qquad \text{Eq. 8}$$

$$f_{\text{stop}}(s_t) = \text{SOFTMAX}\left(m_t\left(\text{AGG}(X)\right)\right) \qquad a_{\text{stop}} \sim f_{\text{stop}}(s_t) \in \backslash\{0,1\backslash\} \qquad \text{Eq. 9}$$

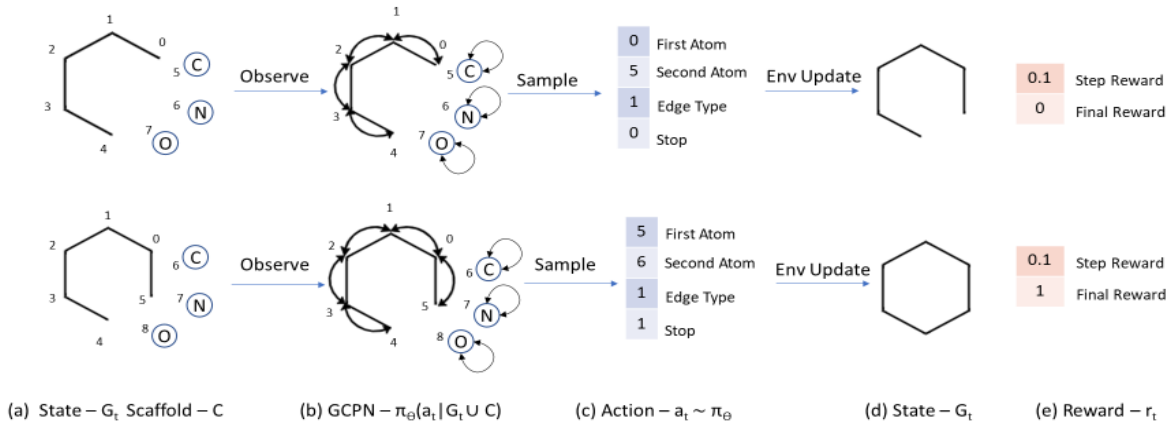

Figure 3. The reinforcement learning pathway for systemic generation of molecules (Redrawn from You *et al*. *[34]*) . (a) The state is defined as the current graph G_t and the possible atom types C. (b) The GCPN conducts message passing to encode the state as node embeddings and estimates the policy function. (c) The action to be performed (a_t) is sampled from the policy function. The environment performs a chemical valency check on the intermediate state and returns (d) the next state G_t and (e) the associated reward (r_t).

2.2.4 Policy Gradient Training

For our experiments, we use Proximal Policy Optimization (PPO) [72], the state-of-the-art policy gradient method, for optimizing the total reward. The objective function for PPO is described in Eq 10.

$$\max L^{\text{CLIP}}(\theta) = \mathbb{E}_t\left[\min\left(r_t(\theta)\hat{A}_t, \text{clip}(r_t(\theta), 1-\epsilon, 1+\epsilon)\hat{A}_t\right)\right]$$

$$r_t(\theta) = \frac{\pi_\theta(a_t|s_t)}{\pi_{\theta_{\text{old}}}(a_t|s_t)} \qquad \text{Eq. 10}$$

$$\hat{A}_t = \delta_t + (\gamma\lambda)\delta_{(t+1)} + \cdots + (\gamma\lambda)^{T-t+1}\delta_{T-1}$$

$$\text{where} \quad \delta_t = R_t + \gamma V(s_{t+1}) - V(s_t)$$

Here s_t, a_t, R_t are the state, action and reward respectively at timestep t, $V(s_t)$ is the value associated with state s_t, π_θ is the policy function and γ is the discount factor. Also note that $\hat{A}_t$, which is an estimator of the advantage function at timestep t, has been estimated using Generalized Advantage Estimation [73] with the GAE parameter λ, since it reduces the variance of the estimate.

For estimating the value of V we use an MLP with the embedding X as the input. Apart from this, we also use expert pretraining [74] which has shown to stabilise the training process. For our experiment, any ground truth molecule can be used as an expert for imitation. We randomly select a subgraph $\hat{G}'$ from the ground truth molecule $\hat{G}$ as the state $\hat{s}_t$. The action $\hat{a}_t$ is also chosen randomly such that it adds an atom or bond in the graph $\hat{G}\backslash\hat{G}'$. This pair ($\hat{s}_t$, $\hat{a}_t$) is used for calculating the expert loss.

$$\min L^{\text{EXPERT}}(\theta) = -\log\left(\pi_\theta(\hat{a}_t|\hat{s}_t)\right) \qquad \text{Eq. 11}$$

Note that we use the same dataset of ground truth molecules for calculating the expert loss and the adversarial rewards. For the rest of the paper, we will call this dataset the "expert dataset" and the random molecule selected from the dataset the "expert molecule".

3. System evaluation

In this section we evaluate the system described above on the task of generating small molecules that interact with the dopamine transporter but not (so far as possible) with the norepinephrine transporter.

3.1 Property Prediction

In this section we evaluate the performance of the supervised property prediction component. Dopamine Transporter binding data was obtained from www.bindingdb.org (https://bit.ly/2YACT5u). The training data consist of some molecules which are labelled with their K_i values and some which are labelled with IC_{50} values. For this paper, we have used IC_{50} values and K_i values interchangeably in order to increase the size of the training dataset. Molecules having large K_i values in the dataset were not labelled accurately (with labels such as ~1000) but the use of a robust loss function allowed us to incorporate these values directly. As stated above we use log transformed values (pKi). (We also attempted to learn the K_i values of the molecules, but the distribution was found to be heteroscedastic; hence we focus on predicting the pK_i values.) Data are shown in Fig 4A for the dopamine transporter and 4B for the norepinephrine transporter pKi values.

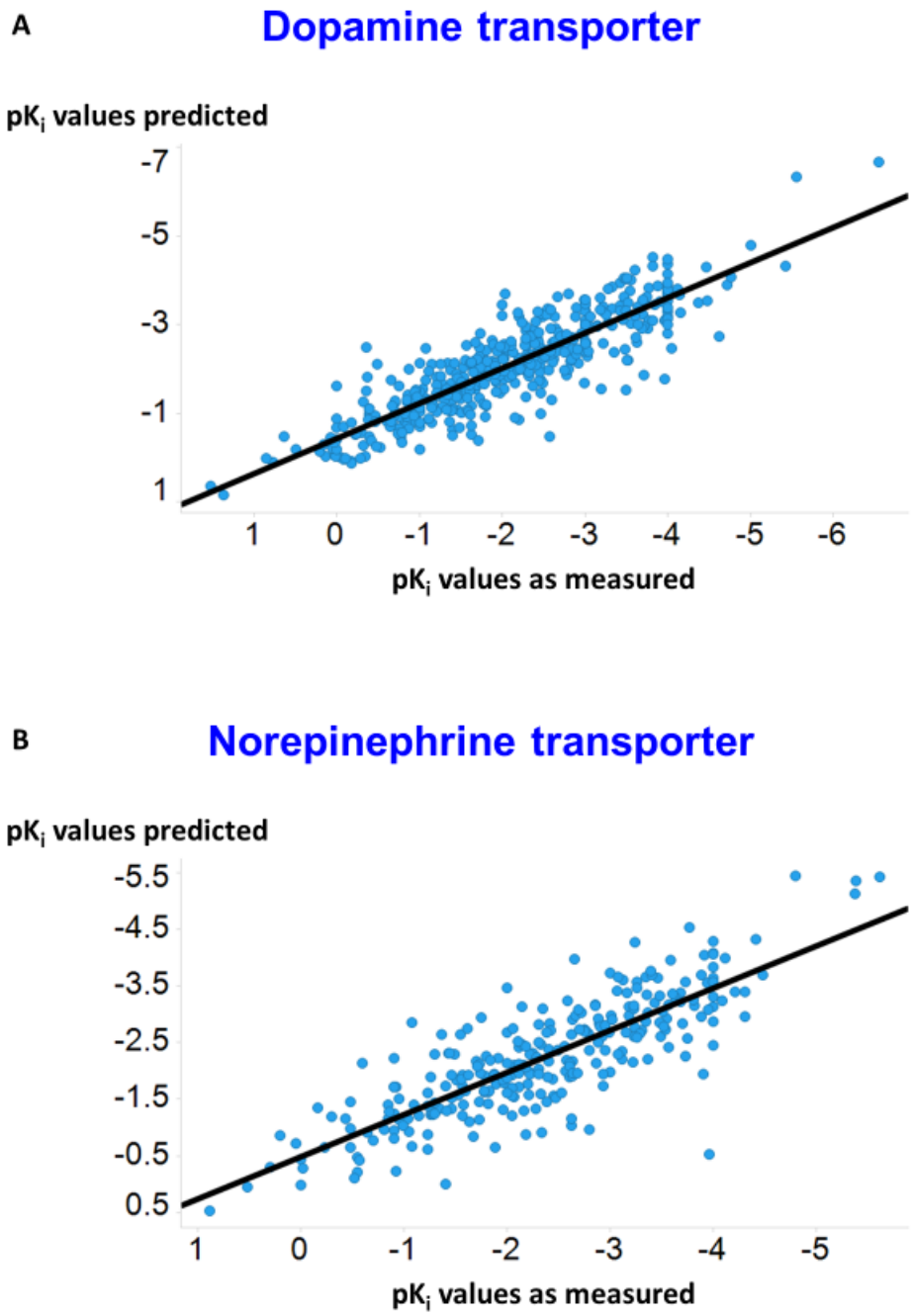

Figure 1 : Predicted and experimental values for the test sets of the dopamine (**A**) and norepinephrine (**B**) transporters. Lines are lines of best fit (**A**: y =0.44 + 0.79x, r^2 = 0.79; **B**: y = 0.49 + 0.74x, r^2 =0.68).

3.1.1 Hyperparameter Optimization

As the property prediction is a general algorithm with a large number of hyperparameters, we attempted to improve generalisation on the transporter problem using Bayesian optimization on the RMSE error between the predicted pKi values and the actual pKi values of the validation set. For this

task we consider the hyperparameters to be the depth of the GCN encoder, the dimensions of the message vectors, the number of layers in the Feed Forward Network, and the Dropout constant.

For the case of the dopamine transporter, the optimum hyperparameters that were obtained are 3 (depth of GCN), 1300 (dimensions of message vector), 2 (FFN layers) and 0.1 (Dropout).The RMS error on the test dataset for the dopamine transporter after Hyperparameter Optimization was found to be 0.57 as compared to an error of 0.65 without it. We attribute this quite significant remaining error to the errors present in the dataset. Similarly for the norepinephrine transporter , the test RMS error was found to be 0.66 after hyperparameter optimization and the optimum hyperparameters obtained are 5 (depth of GCN), 900 (dimensions of message vector), 3 (FFN layers), 0.15 (Dropout).

3.1.2 Implementation details

For the prediction of pKi value of both Dopamine and Norepinephrine transporters, we split the overall dataset into train (80%) , validation (10%) and test (10%) datasets randomly. The training is done with a batch size of 50 molecules and for 100 epochs. All the network weights were initialized using Xavier initialization [75]. The first two epochs are warmup epochs [76] where the learning rate increases from 1e-4 to 1e-3 linearly and after that it decreases exponentially to 1e-4 by the last epoch. The code was written using the PyTorch library and the training was done using an NVIDIA RTX 2080Ti GPU on a Windows 10 system with 256GB RAM and an Intel 18-Core Xeon W-2195 processor.

3.2 Single-Objective Molecular Generation

To begin the RL evaluation we consider molecular generation with a single objective (dopamine transporter interaction). For all the experiments we use the following implementation details. The learning rate for training all the networks is taken to be 1e-3 and linearly decreasing to 0 by 3e7 timesteps. The depth of GCN network for both the GCPN and the Discriminator network is taken to be 3 and the node embedding size was taken to be 128. The code was written using the TensorFlow library and training was done using an NVIDIA RTX 2080Ti GPU

For the task of analysing the results we provide the 'top 10' molecules generated as in Fig 5. However, we aim to generate molecules that are in some sense similar to the original training dataset by systematically modifying the RL pathway in the following experiments. For each experiment, we find the closest molecule in the bindingDB dataset to the top 10 generated molecules. The relative closeness is measured by calculating its Tanimoto Similarity between the RDKit fingerprints, and we visualize the distribution of the TS values.

First, we initialize the molecule with a single Carbon atom in the beginning of the generative process. The expert dataset in this case is chosen to be the ZINC dataset [77], which is a free dataset containing (at that time) some 230M commercially available compounds. However, for our experiments, we use 250K randomly selected molecules from ZINC as our expert dataset to make the experiments computationally tractable. The top generated molecules and their predicted properties are given in Supplementary Table 1 (including data on QED and SA) with a subset of the data illustrated in Fig 5. Note that in all cases the values of QED and SA both exceeded 0.8.

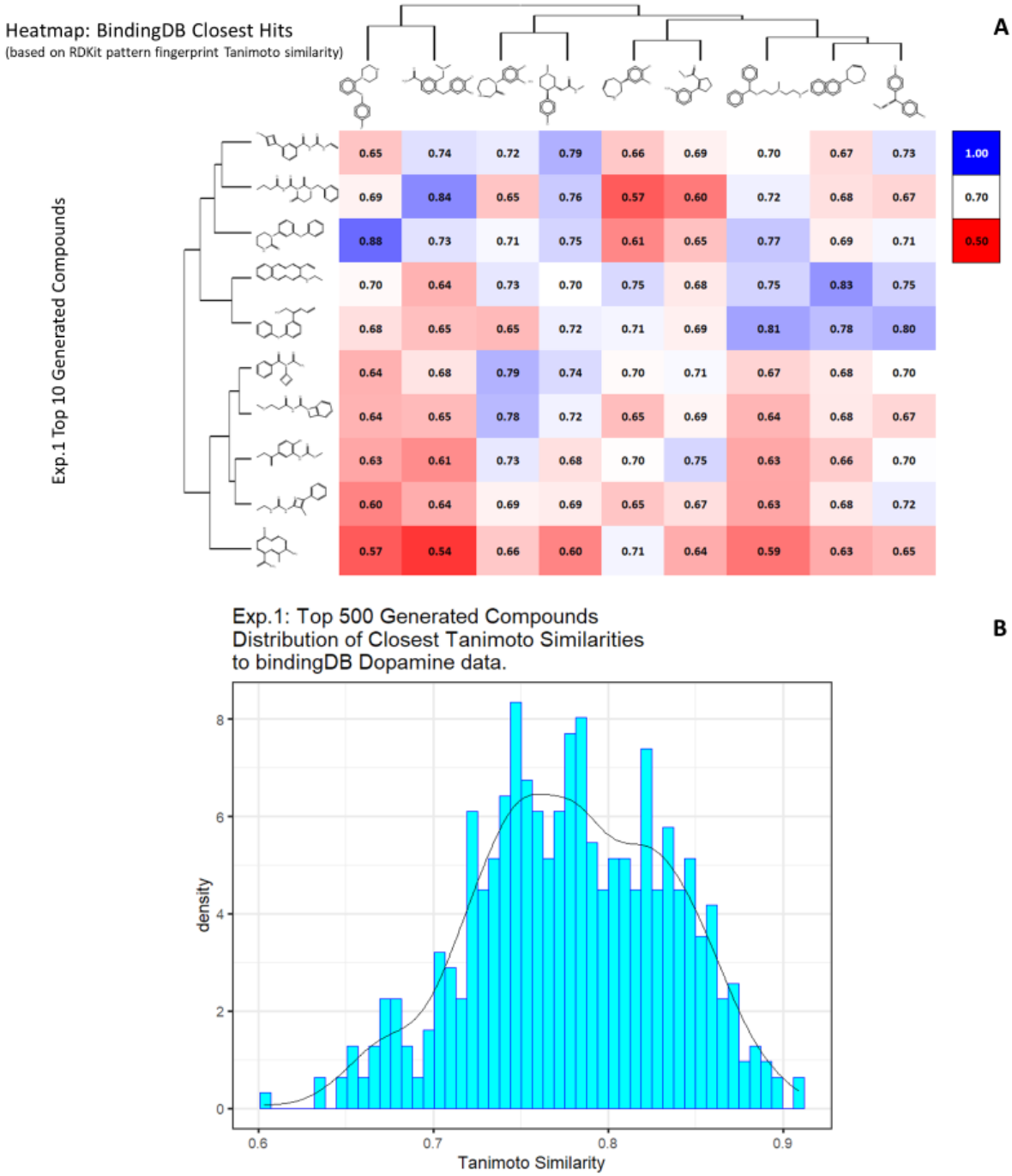

Figure 5. *In silico* generation by DeepGraphMol of novel molecules with predicted binding capacity to the dopamine transporter. Molecules were generated as described in the text. **A.** Top 10 molecules as predicted by DeepGraphMol versus the closest molecule in the BindingdB dataset and the Tanimoto similarity thereto (encoded using the RDKit patterned fingerprint). **B**. Distribution of Tanimoto similarities to a molecule in BindingdB dataset of the top 500 molecules.

Although the above experiment was able to generate optimized molecules, there is no certainty that the predictions are correct due to the errors in the model as well as the errors that were propagated by the experimental errors in the data. We thus attempt to generate molecules that are similar to the more potent molecules. In the next experiment, we choose the expert dataset to be the original

dataset on which we trained the molecules (we will call this the Dopamine Dataset), while omitting molecules having K_i greater than 1000. We again choose the initial molecule to be a single carbon atom. The equivalent data are given in Supplementary Table 2, with similar plots to those of Fig 5 given in Fig 6.

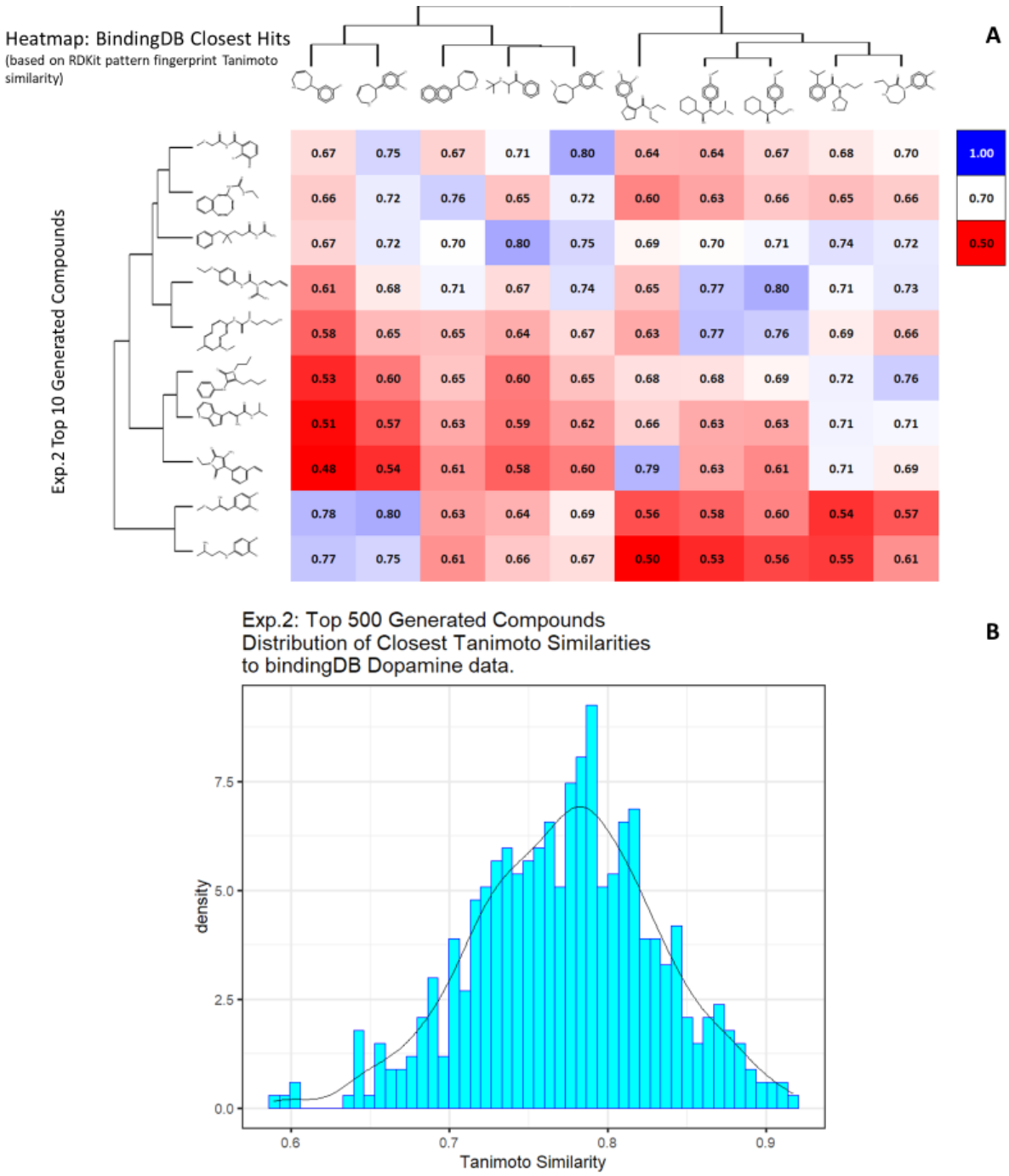

Figure 6. *In silico* generation by DeepGraphMol of novel molecules with predicted binding capacity to the dopamine transporter. Molecules were generated as described in the text. **A.** Top 10 molecules as predicted by DeepGraphMol versus the closest molecule in the BindingdB dataset and the Tanimoto similarity thereto (encoded using the RDKit patterned fingerprint). **B**. Distribution of Tanimoto similarities to a molecule in BindingdB dataset of the top 500 molecules.

Another way to ensure that the generated molecules will have a high affinity towards dopamine transporter is to explicitly ensure that the molecules have higher TS with already known molecules that have high pK_i values. We attempt to achieve this by initializing the generative process with a random molecule from the Dopamine Dataset having Ki < 1000. We conduct two experiments using this process, one where we restrict the number of atoms (other than hydrogen) to be lower than 25 (Supplementary Table 3 and Fig 7), and another (Supplementary Table 4 and Fig 8) where we restrict the number of atoms to be less than 15. For both these experiments, we use the ZINC dataset as the expert dataset. The results are summarized in the tables below. Note that in some cases we obtain a TS of 1; this is encouraging as in this case the algorithm found no need to add anything to the original molecule and could recapitulate it.

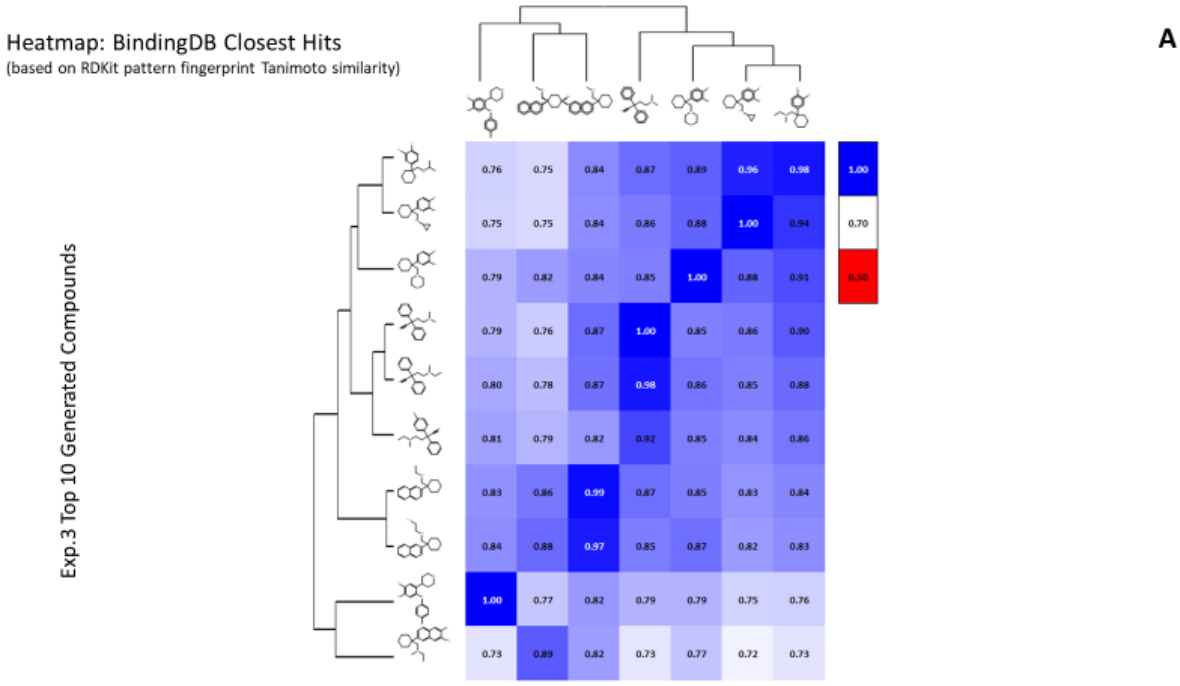

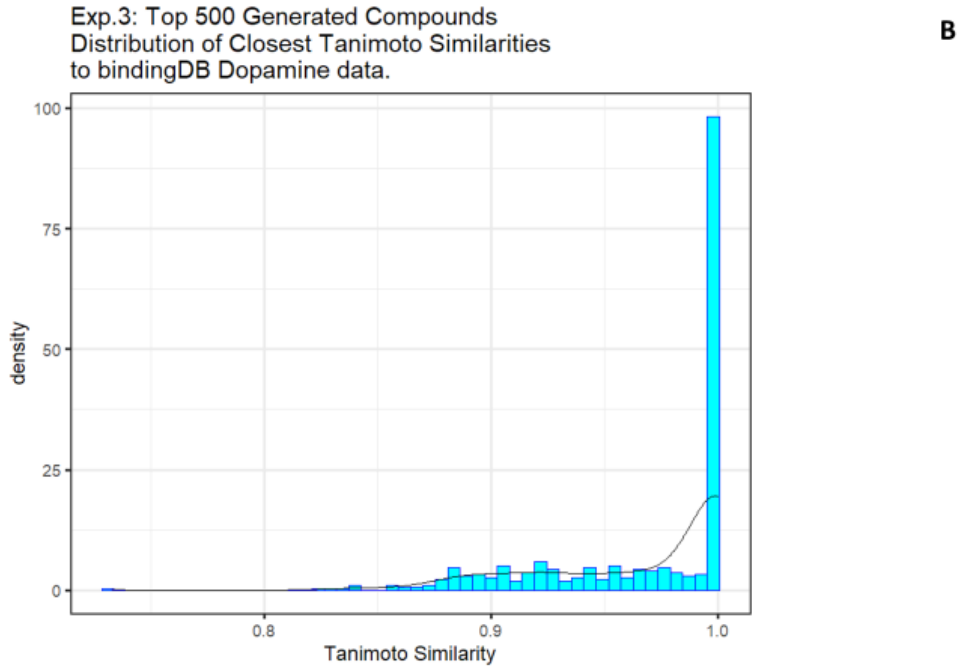

Figure 7. *In silico* generation by DeepGraphMol of novel molecules with predicted binding capacity to the dopamine transporter using a generative method in which the number of heavy atoms is constrained to be lower than 25. Molecules were generated as described in the text. **A.** Top 10 molecules as predicted by DeepGraphMol versus the closest molecule in the BindingdB dataset and the TS thereto (encoded using the RDKit patterned fingerprint). **B**. Distribution of Tanimoto similarities (RDKit patterned encoding) to a molecule in BindingdB dataset of the top 500 molecules.

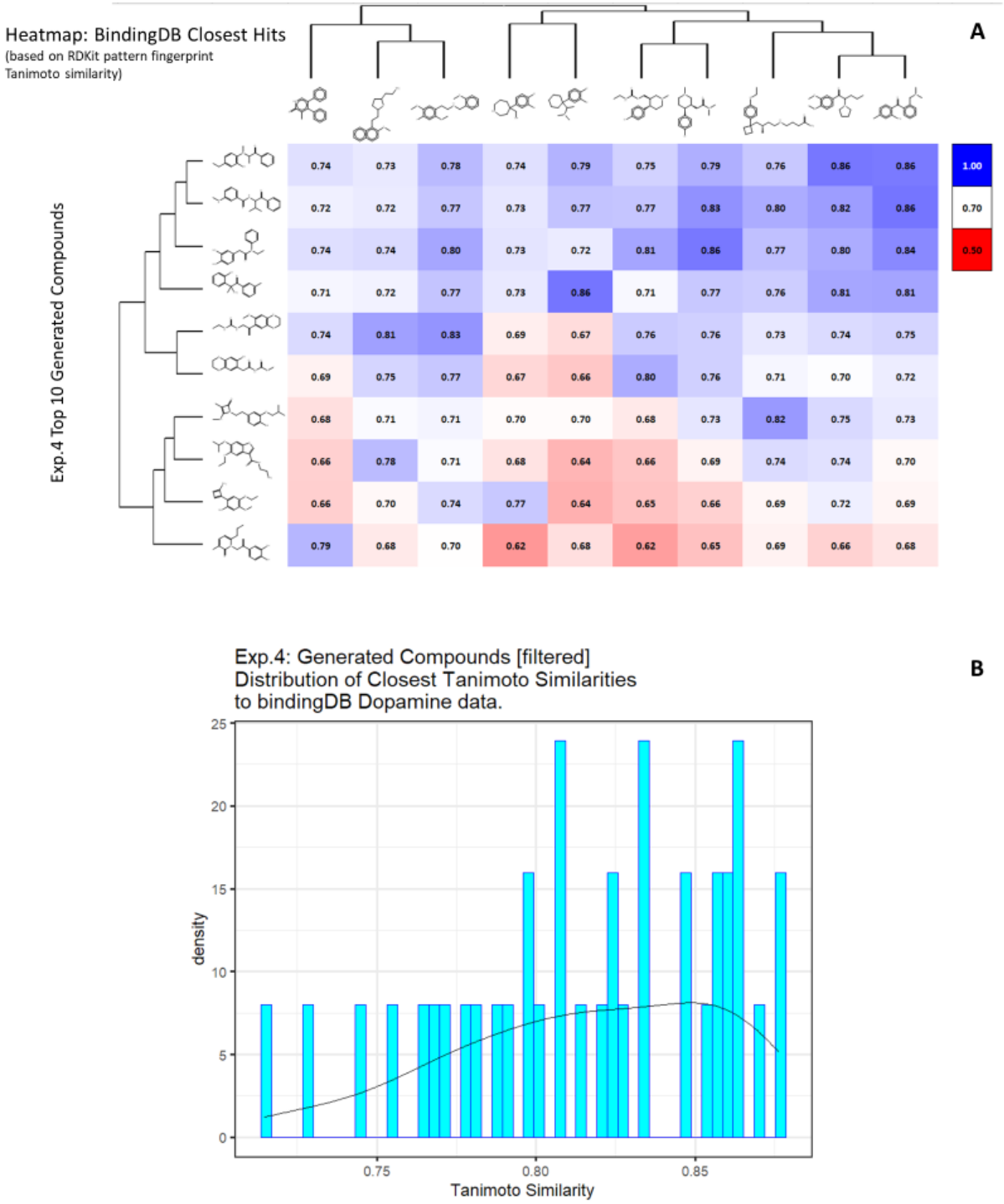

Figure 8. *In silico* generation by DeepGraphMol of novel molecules with predicted binding capacity to the dopamine transporter using a generative method in which the number of heavy atoms is constrained to be lower than 15. Molecules were generated as described in the text. **A.** Top 10

molecules as predicted by DeepGraphMol versus the closest molecule in the BindingdB dataset and the TS thereto (encoded using the RDKit patterned fingerprint). **B**. Distribution of Tanimoto similarities (RDKit patterned encoding) to the closest molecule in BindingdB dataset of the top 500 molecules.

3.3 Multi-Objective Molecular Generation

Even though generating molecules having higher affinity towards a particular ligand in itself is quite sought after, in many cases we might wish to seek molecules that bind to one receptor but explicitly do not bind to another one (kinase inhibitors might be one such example). We attempt to achieve this here with the help of our Reinforcement Learning pipeline by modifying the reward function to be a weighted combination of pK_i values for the two different targets. Explicitly, we attempt to generate molecules that have high binding affinity to the Dopamine Transporter but a much lower binding affinity to the Norepinephrine Transporter. Thus, we modify the reward function used in the previous experiments to add 2 times the predicted pK_i values for Dopamine Transporter and -1 times the predicted pK_i values for the Norepinephrine Transporter. The higher weight is given to the dopamine component since we wish to generate molecules that do bind to it. Clearly we could use any other weightings as part of the reward function, so those chosen are simply illustrative. For this experiment we initialize the process with a random molecule from the Dopamine dataset having a number of atoms lower than 25 and choose the expert dataset to be ZINC. The results of this experiment are summarized in Supplementary Table 5 and Fig 9. As above, some molecules have a TS of 1 in the dataset, for the same reasons.

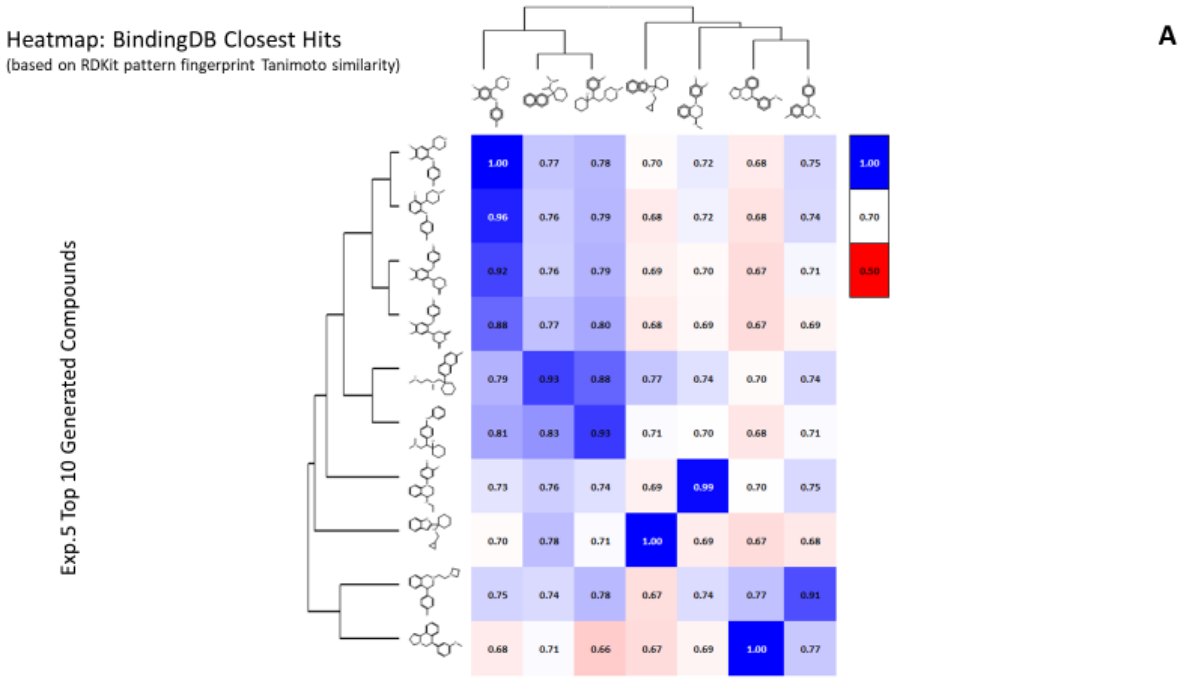

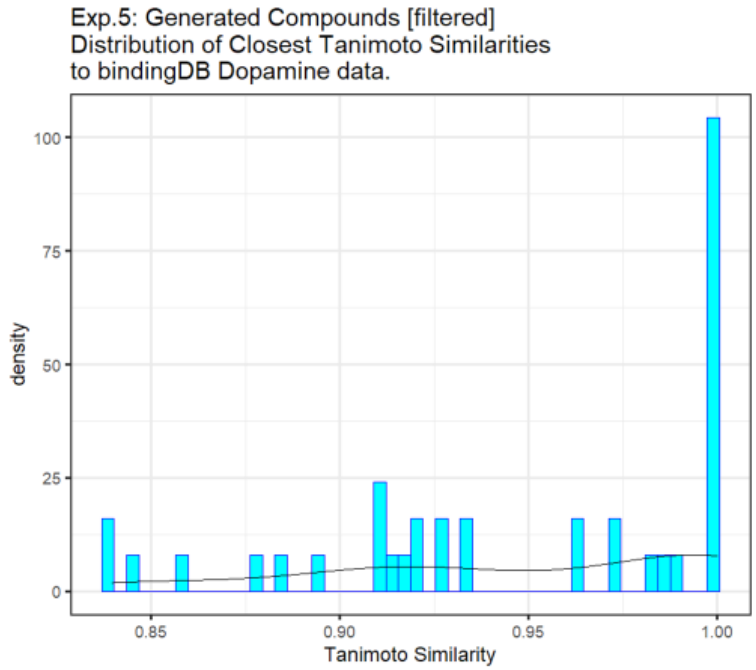

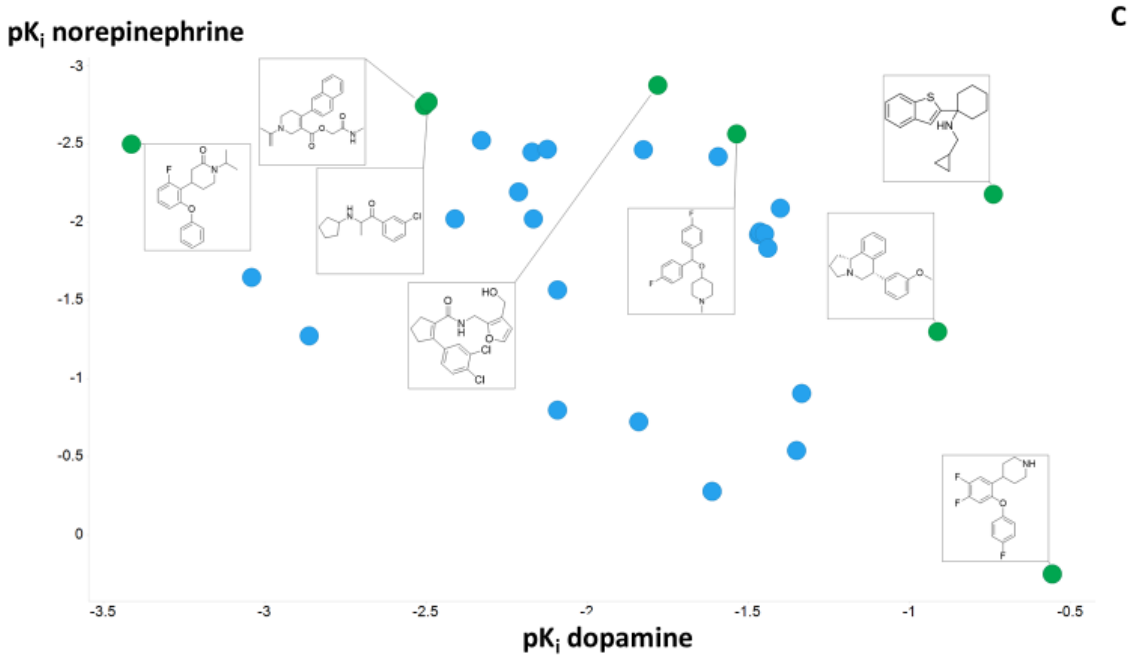

Figure 9. *In silico* generation by DeepGraphMol of novel molecules with predicted binding capacity to the dopamine transporter using a generative method in which the number of heavy atoms is constrained to be lower than 25. Molecules were generated as described in the text. **A.** Top 10 molecules as predicted by DeepGraphMol versus the closest molecule in the BindingdB dataset and the TS thereto (encoded using the RDKit patterned fingerprint). **B**. Distribution of Tanimoto similarities (RDKit patterned encoding) to the closest molecule in BindingdB dataset of the top 500 molecules. **C**. Plot of those molecules with differential affinities for the dopamine and norepinephrine transporters.

Only in rare cases do candidate solutions for multi- (in this case two-)objective optimisation problems have unique solutions that are optimal for both [78], and there is a trade-off that is left to the choice of the experimenter. Thus, Fig 9C also illustrates the molecules on the Pareto front for the two objectives, showing how quite changes in structure can move one swiftly along the Pareto front. Consequently our method also provides a convenient means of attacking multiobjective molecular optimisation problems.

Conclusions

Overall, the present molecular graph-based generative method has a number of advantages over grammar-based encodings, in particular that it necessarily creates valid molecules. As stressed by Coley and colleagues [49], such methods still retain any inherent limitations of 2D methods as *a priori* they do not encode 3D information. This said, there is evidence that 3D structures do not add much benefit when forming QSAR models [79-83], so we do not consider this a major limitation for now. Some of the molecules generated might be seen by some (however subjectively) as 'unusual, even though they scored well on both drug-likeness and synthetic accessibility metrics. This probably says much about the size of plausible drug space that exists relative to the fraction that has actually been explored [84-86], and implies that generative methods can have an important role to play in medicinal chemistry. In conclusion, we here add to the list of useful, generative molecular methods for virtual screening by combining molecular graph encoding, reinforcement learning and multiobjective optimisation within a single strategy.

Acknowledgments

The work of SS and DBK is supported as part of EPSRC grant EP/S004963/1 (SuSCoRD).

Conflict of interest statement

The authors have no conflicts of interest to report.

References

1. Yang X, Zhang J, Yoshizoe K, Terayama K, Tsuda K: **ChemTS: an efficient python library for *de novo* molecular generation**. *Sci Technol Adv Mater* 2017, **18**(1):972-976.
2. Gómez-Bombarelli R, Aguilera-Iparraguirre J, Hirzel TD, Duvenaud D, Maclaurin D, Blood-Forsythe MA, Chae HS, Einzinger M, Ha DG, Wu T *et al*: **Design of efficient molecular organic light-emitting diodes by a high-throughput virtual screening and experimental approach**. *Nat Mater* 2016, **15**(10):1120-+.
3. Gómez-Bombarelli R, Wei JN, Duvenaud D, Hernández-Lobato JM, Sánchez-Lengeling B, Sheberla D, Aguilera-Iparraguirre J, Hirzel TD, Adams RP, Aspuru-Guzik A: **Automatic Chemical Design Using a Data-Driven Continuous Representation of Molecules**. *ACS Cent Sci* 2018, **4**(2):268-276.

4. Sanchez-Lengeling B, Aspuru-Guzik A: **Inverse molecular design using machine learning: Generative models for matter engineering**. *Science* 2018, **361**(6400):360-365.
5. Kadurin A, Nikolenko S, Khrabrov K, Aliper A, Zhavoronkov A: **druGAN: An advanced generative adversarial autoencoder model for *de novo* generation of new molecules with desired molecular properties *in silico***. *Mol Pharm* 2017, **14**(9):3098-3104.
6. Olier I, Sadawi N, Bickerton GR, Vanschoren J, Grosan C, Soldatova L, King RD: **Meta-QSAR: a large-scale application of meta-learning to drug design and discovery**. *Mach Learn* 2018, **107**(1):285-311.
7. Popova M, Isayev O, Tropsha A: **Deep reinforcement learning for *de novo* drug design**. *Sci Adv* 2018, **4**(7):eaap7885.
8. Tabor DP, Roch LM, Saikin SK, Kreisbeck C, Sheberla D, Montoya JH, Dwaraknath S, Aykol M, Ortiz C, Tribukait H *et al*: **Accelerating the discovery of materials for clean energy in the era of smart automation**. *Nature Reviews Materials* 2018, **3**:5-20.
9. Colby SM, Nuñez JR, Hodas NO, Corley CD, Renslow RR: **Deep Learning to Generate in Silico Chemical Property Libraries and Candidate Molecules for Small Molecule Identification in Complex Samples**. *Analytical chemistry* 2020, **92**(2):1720-1729.
10. Baskin, II: **The power of deep learning to ligand-based novel drug discovery**. *Expert Opin Drug Discov* 2020:1-10.
11. Hong SH, Ryu S, Lim J, Kim WY: **Molecular Generative Model Based on an Adversarially Regularized Autoencoder**. *J Chem Inf Model* 2020, **60**(1):29-36.
12. Lim J, Hwang SY, Moon S, Kim S, Kim WY: **Scaffold-based molecular design with a graph generative model**. *Chem Sci* 2020, **11**(4):1153-1164.
13. Rifaioglu AS, Nalbat E, Atalay V, Martin MJ, Cetin-Atalay R, Doğan T: **DEEPScreen: high performance drug-target interaction prediction with convolutional neural networks using 2-D structural compound representations**. *Chem Sci* 2020, **11**(9):2531-2557.
14. Yasonik J: **Multiobjective *de novo* drug design with recurrent neural networks and nondominated sorting**. *J Cheminform* 2020, **12**(1):14.
15. Yoshimori A, Kawasaki E, Kanai C, Tasaka T: **Strategies for Design of Molecular Structures with a Desired Pharmacophore Using Deep Reinforcement Learning**. *Chem Pharm Bull (Tokyo)* 2020, **68**(3):227-233.
16. Walters WP, Murcko M: **Assessing the impact of generative AI on medicinal chemistry**. *Nat Biotechnol* 2020, **38**(2):143-145.
17. Griffiths RR, Hernández-Lobato JM: **Constrained Bayesian optimization for automatic chemical design using variational autoencoders**. *Chem Sci* 2020, **11**(2):577-586.
18. Cova TFGG, Pais AACC: **Deep Learning for Deep Chemistry: Optimizing the Prediction of Chemical Patterns**. *Front Chem* 2019, **7**.
19. Noh J, Kim J, Stein HS, Sanchez-Lengeling B, Gregoire JM, Aspuru-Guzik A, Jung Y: **Inverse Design of Solid-State Materials via a Continuous Representation**. *Matter* 2019, **1**(5):1370-1384.
20. Grisoni F, Schneider G: ***De novo* Molecular Design with Generative Long Short-term Memory**. *Chimia* 2019, **73**(12):1006-1011.
21. Grisoni F, Merk D, Friedrich L, Schneider G: **Design of Natural-Product-Inspired Multitarget Ligands by Machine Learning**. *ChemMedChem* 2019, **14**(12):1129-1134.
22. Gupta A, Müller AT, Huisman BJH, Fuchs JA, Schneider P, Schneider G: **Generative Recurrent Networks for *de novo* drug design**. *Mol Inform* 2018, **37**(1-2).
23. Merk D, Friedrich L, Grisoni F, Schneider G: **De Novo Design of Bioactive Small Molecules by Artificial Intelligence**. *Mol Inform* 2018, **37**(1-2).
24. Schneider G: **Generative models for artificially-intelligent molecular design**. *Mol Inform* 2018, **37**(1-2):188031.

25. Schneider P, Walters WP, Plowright AT, Sieroka N, Listgarten J, Goodnow RA, Fisher J, Jansen JM, Duca JS, Rush TS *et al*: **Rethinking drug design in the artificial intelligence era**. *Nat Rev Drug Discov* 2020, **19**:353-364.
26. Button A, Merk D, Hiss JA, Schneider G: **Automated *de novo* molecular design by hybrid machine intelligence and rule-driven chemical synthesis**. *Nat mach Intell* 2019, **1**(7):307-315.
27. Moret M, Friedrich L, Grisoni F, Merk D, Schneider G: **Generative molecular design in low data regimes**. *Nat Mach Intell* 2020, **2**:171-180.
28. Ståhl N, Falkman G, Karlsson A, Mathiason G, Boström J: **Deep Reinforcement Learning for Multiparameter Optimization in *de novo* Drug Design**. *J Chem Inf Model* 2019, **59**(7):3166-3176.
29. Arús-Pous J, Blaschke T, Ulander S, Reymond JL, Chen H, Engkvist O: **Exploring the GDB-13 chemical space using deep generative models**. *J Cheminform* 2019, **11**(1):20.
30. Reymond JL: **The Chemical Space Project**. *Acc Chem Res* 2015, **48**(3):722-730.
31. Bohacek RS, McMartin C, Guida WC: **The art and practice of structure-based drug design: A molecular modeling perspective**. *Med Res Rev* 1996, **16**(1):3-50.
32. Ertl P: **Cheminformatics analysis of organic substituents: identification of the most common substituents, calculation of substituent properties, and automatic identification of drug-like bioisosteric groups**. *J Chem Inf Comput Sci* 2003, **43**(2):374-380.
33. O'Hagan S, Kell DB: **Analysing and navigating natural products space for generating small, diverse, but representative chemical libraries**. *Biotechnol J* 2018, **13**(1):1700503.
34. You J, Liu B, Ying R, Pande V, Leskovec J: **Graph Convolutional Policy Network for Goal-Directed Molecular Graph Generation**. *arXiv* 2018:1806.02473v02471.
35. Dimova D, Stumpfe D, Bajorath J: **Method for the Evaluation of Structure-Activity Relationship Information Associated with Coordinated Activity Cliffs**. *J Med Chem* 2014.
36. Stumpfe D, Hu Y, Dimova D, Bajorath J: **Recent progress in understanding activity cliffs and their utility in medicinal chemistry**. *J Med Chem* 2014, **57**(1):18-28.
37. Stumpfe D, Dimova D, Bajorath J: **Composition and topology of activity cliff clusters formed by bioactive compounds**. *J Chem Inf Model* 2014, **54**(2):451-461.
38. Teixeira AL, Leal JP, Falcao AO: **Random forests for feature selection in QSPR Models - an application for predicting standard enthalpy of formation of hydrocarbons**. *J Cheminform* 2013, **5**(1):9.
39. Ambure P, Halder AK, Gonzalez Diaz H, Cordeiro M: **QSAR-Co: An Open Source Software for Developing Robust Multitasking or Multitarget Classification-Based QSAR Models**. *J Chem Inf Model* 2019, **59**(6):2538-2544.
40. Zupan J, Gasteiger J: **Neural Networks for Chemists**. Weinheim: Verlag Chemie; 1993.
41. Livingstone D: **Data analysis for chemists**. Oxford: Oxford University Press; 1995.
42. Mahé P, Vert JP: **Virtual screening with support vector machines and structure kernels**. *Comb Chem High Throughput Screen* 2009, **12**(4):409-423.
43. O'Hagan S, Kell DB: **The KNIME workflow environment and its applications in Genetic Programming and machine learning**. *Genetic Progr Evol Mach* 2015, **16**:387-391.
44. LeCun Y, Bengio Y, Hinton G: **Deep learning**. *Nature* 2015, **521**(7553):436-444.
45. Schmidhuber J: **Deep learning in neural networks: an overview**. *Neural Netw* 2015, **61**:85-117.
46. Gawehn E, Hiss JA, Schneider G: **Deep learning in drug discovery**. *Mol Inform* 2016, **35**(1):3-14.
47. Ching T, Himmelstein DS, Beaulieu-Jones BK, Kalinin AA, Do BT, Way GP, Ferrero E, Agapow PM, Zietz M, Hoffman MM *et al*: **Opportunities and obstacles for deep learning in biology and medicine**. *J R Soc Interface* 2018, **15**(141).
48. Mater AC, Coote ML: **Deep Learning in Chemistry**. *J Chem Inf Model* 2019, **59**(6):2545-2559.

49. Coley CW, Barzilay R, Green WH, Jaakkola TS, Jensen KF: **Convolutional Embedding of Attributed Molecular Graphs for Physical Property Prediction**. *J Chem Inf Model* 2017, **57**(8):1757-1772.
50. Weininger D: **SMILES, a chemical language and information system .1. Introduction to methodology and encoding rules**. *J Chem Inf Comput Sci* 1988, **28**(1):31-36.
51. Dai H, Tian Y, Dai B, Skiena S, Song L: **Syntax-directed variational autoencoder for structured data**. *arXiv* 2018:1802.08786v08721.
52. Kusner MJ, Paige B, Hernández-Lobato JM: **Grammar Variational Autoencoder**. *arXiv* 2017:1703.01925v01921.
53. Blaschke T, Olivecrona M, Engkvist O, Bajorath J, Chen HM: **Application of generative autoencoder in *de novo* molecular design**. *Mol Inform* 2018, **37**(1-2):1700123.
54. Xu Y, Lin K, Wang S, Wang L, Cai C, Song C, Lai L, Pei J: **Deep learning for molecular generation**. *Future Med Chem* 2019, **11**(6):567-597.
55. O'Boyle N, Dalke A: **DeepSMILES: An Adaptation of SMILES for Use in Machine-Learning of Chemical Structures**. *ChemRxiv* 2018:7097960.v7097961.
56. Goodfellow I, Bengio Y, Courville A: **Deep learning**. Boston: MIT Press; 2016.
57. Stokes JM, Yang K, Swanson K, Jin W, Cubillos-Ruiz A, Donghia NM, MacNair CR, French S, Carfrae LA, Bloom-Ackerman Z *et al*: **A Deep Learning Approach to Antibiotic Discovery**. *Cell* 2020, **180**(4):688-702 e613.
58. Zahoránszky-Kőhalmi G, Bologa CG, Oprea TI: **Impact of similarity threshold on the topology of molecular similarity networks and clustering outcomes**. *J Cheminform* 2016, **8**:16.
59. Segler MHS, Kogej T, Tyrchan C, Waller MP: **Generating Focussed Molecule Libraries for Drug Discovery with Recurrent Neural Networks**. *arXiv* 2017:1701.01329v01321.
60. O'Hagan S, Kell DB: **Consensus rank orderings of molecular fingerprints illustrate the 'most genuine' similarities between marketed drugs and small endogenous human metabolites, but highlight exogenous natural products as the most important 'natural' drug transporter substrates.** *ADMET & DMPK* 2017, **5**(2):85-125.
61. Kajino H: **Molecular Hypergraph Grammar with Its Application to Molecular Optimization**. *arXiv* 2018:1809.02745v02741.
62. Jin W, Barzilay R, Jaakkola T: **Junction Tree Variational Autoencoder for Molecular Graph Generation**. *arXiv* 2018:1802.04364v04362.
63. Bickerton GR, Paolini GV, Besnard J, Muresan S, Hopkins AL: **Quantifying the chemical beauty of drugs**. *Nat Chem* 2012, **4**(2):90-98.
64. Zhang Z, Cui P, Zhu W: **Deep learning on graphs: a survey**. *arXiv* 2018:1812.04202v04201.
65. Barron JT: **A General and Adaptive Robust Loss Function**. *arXiv* 2017:1701.03077v03010.
66. Yang K, Swanson K, Jin W, Coley C, Eiden P, Gao H, Guzman-Perez A, Hopper T, Kelley B, Mathea M *et al*: **Analyzing Learned Molecular Representations for Property Prediction**. *arXiv* 2019:1904.01561v01564.
67. Yang K, Swanson K, Jin W, Coley C, Eiden P, Gao H, Guzman-Perez A, Hopper T, Kelley B, Mathea M *et al*: **Analyzing Learned Molecular Representations for Property Prediction**. *J Chem Inf Model* 2019, **59**(8):3370-3388.
68. Goodacre R, Trew S, Wrigley-Jones C, Saunders G, Neal MJ, Porter N, Kell DB: **Rapid and quantitative analysis of metabolites in fermentor broths using pyrolysis mass spectrometry with supervised learning: application to the screening of *Penicillium chryosgenum* fermentations for the overproduction of penicillins.** *Anal Chim Acta* 1995, **313**:25-43.
69. Jarrett K, Kavukcuoglu K, Ranzato M, Lecun Y: **What is the Best Multi-Stage Architecture for Object Recognition?** *Ieee I Conf Comp Vis* 2009:2146-2153.
70. Ashkezari-Toussi S, Sadoghi-Yazdi H: **Robust diffusion LMS over adaptive networks**. *Signal Process* 2019, **158**:201-209.
71. Ertl P, Schuffenhauer A: **Estimation of synthetic accessibility score of drug-like molecules based on molecular complexity and fragment contributions**. *J Cheminform* 2009, **1**(1):8.

72. Schulman J, Wolski F, Dhariwal P, Radford A, Klimov O: **Proximal Policy Optimization Algorithms**. *arXiv* 2017:1707.06347v06342.
73. Schulman J, Moritz P, Levine S, Jordan M, Abbeel P: **High-Dimensional Continuous Control Using Generalized Advantage Estimation**. *arXiv* 2015:1506.02438.
74. Levine S, Koltun V: **Guided policy search.** *Proc ICML* 2013, **28**:1-9.
75. Glorot X, Bengio Y: **Understanding the difficulty of training deep feedforward neural networks**. *Proc AISTATs* 2010, **9**:249-256.
76. Li Y, Wei C, Ma T: **Towards Explaining the Regularization Effect of Initial Large Learning Rate in Training Neural Networks**. *arXiv* 2019:1907.04595v04592.
77. Sterling T, Irwin JJ: **ZINC 15 - Ligand Discovery for Everyone**. *J Chem Inf Model* 2015, **55**:2324-2337.
78. Besnard J, Ruda GF, Setola V, Abecassis K, Rodriguiz RM, Huang XP, Norval S, Sassano MF, Shin AI, Webster LA *et al*: **Automated design of ligands to polypharmacological profiles**. *Nature* 2012, **492**(7428):215-220.
79. Nettles JH, Jenkins JL, Bender A, Deng Z, Davies JW, Glick M: **Bridging chemical and biological space: "target fishing" using 2D and 3D molecular descriptors**. *J Med Chem* 2006, **49**(23):6802-6810.
80. Hu G, Kuang G, Xiao W, Li W, Liu G, Tang Y: **Performance evaluation of 2D fingerprint and 3D shape similarity methods in virtual screening**. *J Chem Inf Model* 2012, **52**(5):1103-1113.
81. Oprea TI: **On the information content of 2D and 3D descriptors for QSAR**. *J Brazil Chem Soc* 2002, **13**(6):811-815.
82. Brown RD, Martin YC: **The information content of 2D and 3D structural descriptors relevant to ligand-receptor binding**. *J Chem Inf Comp Sci* 1997, **37**(1):1-9.
83. Hong HX, Xie Q, Ge WG, Qian F, Fang H, Shi LM, Su ZQ, Perkins R, Tong WD: **Mold^2, molecular descriptors from 2D structures for chemoinformatics and toxicoinformatics**. *J Chem Inf Model* 2008, **48**(7):1337-1344.
84. Hann MM, Keserü GM: **Finding the sweet spot: the role of nature and nurture in medicinal chemistry**. *Nat Rev Drug Discov* 2012, **11**(5):355-365.
85. Pitt WR, Parry DM, Perry BG, Groom CR: **Heteroaromatic Rings of the Future**. *J Med Chem* 2009, **52**:2952-2963.
86. Roughley SD, Jordan AM: **The medicinal chemist's toolbox: an analysis of reactions used in the pursuit of drug candidates**. *J Med Chem* 2011, **54**(10):3451-3479.